

1 **Cell viability in three *ex vivo* rat models of spinal cord injury**

2

3 RUNNING TITLE: Cell viability in *ex vivo* SCI models

4

5 AUTHOR(S): Azim Patar^{1,4}, Peter Dockery², Linda Howard^{3β}, Siobhan S. McMahon^{1β*}

6

7 AFFILIATION(S): ¹Discipline of Anatomy and NCBES Galway Neuroscience Centre, College
8 of Medicine Nursing and Health Sciences, National University of Ireland Galway, Ireland;

9 ²Discipline of Anatomy, College of Medicine Nursing and Health Sciences, National University
10 of Ireland Galway, Ireland; ³Regenerative Medicine Institute (REMEDI), College of Medicine
11 Nursing and Health Sciences, National University of Ireland Galway, Ireland; ⁴Department of
12 Neuroscience, School of Medical Sciences, Universiti Sains Malaysia, Malaysia

13

14 ^βLinda Howard and Siobhan S. McMahon should be considered joint senior authors

15

16 *CORRESPONDING AUTHOR: Dr Siobhan McMahon, Discipline of Anatomy and NCBES
17 Galway Neuroscience Centre, College of Medicine Nursing and Health Sciences, National
18 University of Ireland Galway, Ireland. EMAIL: siobhan.mcmahon@nuigalway.ie TEL: +353
19 91492838. FAX: Fax: +353 91 494520

20

21

22

23 **ABSTRACT**

24 Spinal cord injury (SCI) is a devastating disorder that has poor prognosis of recovery. Animal
25 models of SCI are useful to understand the pathophysiology of SCI and the potential use of
26 therapeutic strategies for human SCI. *Ex vivo* models of central nervous system (CNS) trauma,
27 particularly mechanical trauma, have become important tools to compliment *in vivo* models of
28 injury in order to reproduce the sequelae of human CNS injury. *Ex vivo* organotypic slice cultures
29 (OSCs) provide a reliable model platform for the study of cell dynamics and therapeutic
30 intervention following SCI. In addition, these *ex vivo* models support the 3R's concept of
31 replacement, reduction and refinement of animal use in SCI research. *Ex vivo* models cannot be
32 used to monitor functional recovery, nor do they have the intact blood supply of the *in vivo* model
33 systems. However, the *ex vivo* models appear to reproduce many of the post traumatic events
34 including acute and secondary injury mechanisms. Several well-established OSC models have
35 been developed over the past few years for experimental spinal injuries *ex vivo* in order to
36 understand the biological response to injury. In this study we investigated cell viability in three
37 *ex vivo* OSC models of SCI: stab injury, transection injury and contusion injury. Injury was
38 inflicted in postnatal day 4 rat spinal cord slices. Stab injury was performed using a needle on
39 transverse slices of spinal cord. Transection injury was performed on longitudinal slices of spinal
40 cord using a double blade technique. Contusion injury was performed on longitudinal slices of
41 spinal cord using an Infinite Horizon impactor device. At days 3 and 10 post-injury, viability was
42 measured using dual staining for Propidium Iodide (PI) and Fluorescein Diacetate (FDA). In all
43 *ex vivo* SCI models, the slices showed more live cells than dead cells over 10 days in culture, with
44 higher cell viability in control slices compared to injured slices. Although no change in cell

45 viability was observed between time points in stab and contusion injured OSCs; a reduction in cell
46 viability was observed over time in transection injured OSCs. Taken together, *ex vivo* SCI models
47 are a useful and reliable research tool that reduces the cost and time involved in carrying out animal
48 studies. The use of OSC models provide a simple way to study the cellular consequences following
49 SCI and they can also be used to investigate potential therapeutics regimes for the treatment of
50 SCI.

51

52 **KEYWORDS:** *Ex vivo* slice culture, spinal cord injury, stab injury, transection injury, contusion
53 injury, cell viability

54

55

56 INTRODUCTION

57 Cell death is one of the consequences of traumatic SCI, with both neurons and supporting glial
58 cells affected (Beattie *et al.*, 2002). Numerous studies have reported spinal cord tissue samples
59 isolated from embryonic or newborn rats (Sypecka *et al.*, 2015, Pohland *et al.*, 2015, Weightman
60 *et al.*, 2014, Hashemian *et al.*, 2014, Gerardo-Nava *et al.*, 2014, Pinkernelle *et al.*, 2013, Gerardo-
61 Nava *et al.*, 2013, Ravikumar *et al.*, 2012, Kim *et al.*, 2010, Cho *et al.*, 2009, Krassioukov *et al.*,
62 2002). The organotypic slice culture (OSC) model appears to reproduce much of the post traumatic
63 events following injury including acute and secondary injury mechanisms. It has been reported
64 that there is a significant difference in function, circuitry connections and regenerative capacities
65 in the immature spinal cord compared to adult (Krassioukov *et al.*, 2002). The heterogeneous
66 populations of cells found *in vivo* are maintained within OSCs with three dimensional connections
67 between neurons and supporting cells (Pohland *et al.*, 2015, Pellowaska *et al.*, 2015, Weightman *et*
68 *al.*, 2014, Hashemian *et al.*, 2014, Gerardo-Nava *et al.*, 2014, Pinkernelle *et al.*, 2013, Gerardo-
69 Nava *et al.*, 2013, Ravikumar *et al.*, 2012, Kim *et al.*, 2010, Cho *et al.*, 2009) to avoid hypoxia and
70 necrosis of the central tissue (Krassioukov *et al.*, 2002).

71 A SCI caused by a stab injury is a rare type of injury in patients, resulting in partial or, in
72 some rare cases, the complete transection of the spinal cord (O'Neill *et al.*, 2004). The reproducible
73 way to model a spinal cord stab injury is to cut the corticospinal tract (CST) at the dorsal column
74 of the spinal cord using a sharp object (Suzuki *et al.*, 2010). The stab injury of the dorsal CST
75 results in loss of locomotion of hind limbs and depending on the level of the injury, forelimbs can
76 also be affected (McCaughey *et al.*, 2016, O'Neill *et al.*, 2004). Transection injury of the spinal
77 cord is rarely encountered in clinical practice, however it is a widely used SCI model because it is
78 a reproducible and reliable model for investigation of regeneration, degeneration, neuroplasticity

79 and tissue engineering applications (Cheriyān *et al.*, 2014). Two types of transection injury are
80 commonly used in animal models of SCI: full transection and partial transection (hemisection
81 injury). Since the injury model is easy to perform and is reproducible, this injury model has been
82 reported in a variety of species including rat, mice, cats, dogs and primates (Cheriyān *et al.*, 2014).
83 The contusion injury model is the most clinically relevant model of SCI and is commonly used in
84 animal models of SCI (Adamchik *et al.*, 2000, Krassioukov *et al.*, 2002, Sieg *et al.*, 1999). This
85 injury model is similar to the compressive trauma method *in vitro*, however this method utilises
86 dropping a weight from the prescribed height onto organotypic cultures of spinal cord. The
87 severity of the impact is in proportion to the mass of the weight and the height of the drop. A
88 recent study reported by Krassioukov *et al* (2002) used a pin drop that weighed 0.2g and was
89 dropped from 1.7 cm height onto the centre of OSC slices. Other studies have used similar weight
90 drop apparatus in OSC of brain tissue (Adamchik *et al.*, 2000, Sieg *et al.*, 1999). These *in vitro*
91 weight drop models bear some resemblance to the models used in *in vivo* SCI in rats and mice, i.e.
92 the New York University (NYU) Impactor, Infinite horizon (IH) and Ohio State University (OSU)
93 Impactor (Cheriyān *et al.*, 2014).

94 The viability of cells in organotypic cultures is a very important parameter to consider
95 when culturing *ex vivo* slice cultures as this indicates the health of the tissue slices. The
96 investigation of live and dead cells described in this manuscript can be tested using a simple cell
97 viability assay. Dual staining using a live and dead assay containing Fluorescein Diacetate (FDA)
98 and Propidium Iodide (PI) was used in this study to examine cell viability within spinal cord slices
99 over 10 days in culture. The time window was chosen as day 3 and 10 post-injury in this study
100 due to most secondary mechanism events of cell death following *ex vivo* occurred at this time
101 window (Cho *et al.*, 2009). A slightly longer period of time was used by Gerardo-Nava (2014)

102 who kept the slices in culture between 7-14 days to investigate the interaction between axons in
103 postnatal spinal cord. Slice thickness of the spinal cord tissue is recommended at 350–400µm as
104 this has been reported to avoid hypoxia and necrosis of the central tissue (Krassioukov et al., 2002).
105 In this study, two different spinal cord slice orientations were chosen, transverse and longitudinal.
106 The slice orientation cut for stab injury was transverse due to the clear visibility of dorsal white
107 matter in this orientation versus longitudinal slices. In the transverse slices we aimed to create a
108 stab injury at the CST in the dorsal white matter and it is much easier to observe the CST in
109 transverse slices (Suzuki et al., 2010). For transection and contusion induced injury, a longitudinal
110 slice orientation was chosen as this is a suitable orientation for disruption of the long axons that
111 extend along the long axis of the cord and also to observe the mixed population of cells in grey
112 and white matter of spinal cords.

113 The aim of this study was to develop reproducible *ex vivo* models of SCI and compare the
114 cell viability of the spinal cord slices. In this paper, we described the development of three *ex vivo*
115 OSC models of SCI: stab injury, transection injury and contusion injury. We attempt to mimic
116 injury models *in vivo* by refining these *ex vivo* organotypic spinal culture and carried out the
117 investigation on the viability of the OSCs using dual staining of PI and FDA.

118

119 **MATERIALS AND METHODS**

120 **Animals**

121 Sprague-Dawley rats (Charles River UK Ltd, Margate, UK) were used in this study. All housing
122 and surgical procedures carried out in this study were approval by the Animal Care Research Ethics
123 Committee (ACREC) at the National University of Ireland Galway. Postnatal day (P) 4 rat pups

124 were sacrificed by anaesthesia with 5% Isoflurane followed by decapitation using a guillotine
125 (Stoelting Co, Germany). The bodies were kept in sterile dishes on ice prior to spinal cord
126 harvesting. Spinal cord isolation was performed in a class II biological safety cabinet under aseptic
127 conditions. The skin was incised using a sterile blade #10 (Swann-Morton, England) along the
128 midline of the dorsum. A small transverse incision was made on the sacral vertebrae. The spinal
129 cords were flushed from the vertebral column using a 1ml syringe fitted with an 18G needle and
130 filled with 1X ice-cold Phosphate Buffered Saline (PBS; pH 7.4) (Kennedy *et al.*, 2013). The
131 spinal cords were suspended in ice-cold artificial cerebrospinal fluid (aCSF; pH 7.4) composed of
132 126mM NaCl, 2.5mM KCl, 1.25mM NaH₂PO₄.H₂O, 2mM CaCl₂.2H₂O, 2mM MgSO₄.7H₂O and
133 10mM glucose (all from Sigma Aldrich, Ireland). The meninges was gently dissected away using
134 sterile fine forceps in ice-cold aCSF using a stereomicroscope (Wild MZ32, Switzerland). The
135 intact spinal cords were cut into smaller segments (approximately 1 cm). Three different spinal
136 cord injury models were carried out on the spinal cords after they were chopped on a tissue
137 chopper: stab injury, transection injury and contusion injury. For each injury model, spinal cords
138 were isolated from three litters of P4 rat pups (average litter size 12 pups per litter). For each
139 injury model, the information below details the experiment performed when using one litter.

140

141 **Spinal cord stab injury model**

142 Transverse sections of spinal cord were chopped at 350 µm thickness on the McIlwain tissue
143 chopper (Mickle Laboratory Engineering Co. Ltd., USA) and tissue slices were pooled together in
144 a petri dish containing aCSF. The tissue slices were then transferred to 30mm diameter cell culture
145 inserts (Merck Millipore, Germany) and cultured in 6 well trays (5 slices per insert). Slices were

146 maintained in 1ml of spinal cord slice culture medium consisting of: 48% MEM, 25 mM Hepes,
147 25% heat-inactivated horse serum, 2 mM glutamine, 1% Penicillin Streptomycin, 1% N-Acetyl L-
148 Cystein and 25% Hanks Balanced Salt Solution (all from Sigma Aldrich, Ireland) at 37°C in a 5%
149 humidified CO₂ atmosphere. After 4 days in culture, the tissue slices were separated into a control
150 (uninjured; 6 spinal cord tissue transverse slices) and an injury group (6 spinal cord tissue
151 transverse slices). A stab injury was created in the slices within the injury group using a sterile
152 27G needle targeting the corticospinal tract of the slices located within the dorsal white matter.
153 The anatomical region of the rat corticospinal tract/dorsal white matter region was defined based
154 on the proportion of white matter and gray matter in the transverse slices observed using the
155 stereomicroscope (Steward and Willenberg, 2017). At 3 days and 10 days post injury, medium
156 was aspirated from culture wells and the slices were fixed with 4% paraformaldehyde (PFA) for
157 24 hours at 4°C (3 spinal cord tissue slices per time point in the control group and 3 spinal cord
158 tissue slices per time point in the injured group).

159

160 **Spinal cord transection injury model**

161 Longitudinal sections of spinal cord were chopped at 350 µm thickness using the McIlwain tissue
162 chopper. All tissue slices were pooled together in a petri dish. The spinal cord tissue slices were
163 then transferred to 30 mm diameter cell culture inserts (Merck Millipore, Germany). Two slices
164 per insert were cultured at 37°C in a 5% humidified CO₂ atmosphere in 6 well trays containing
165 1ml spinal cord slice culture medium (see preceding section for list of culture medium
166 ingredients). After 4 days in culture, the tissue slices were separated into a control group
167 (uninjured, 6 slices) and injured group (6 slices). A transection injury was performed on the spinal

168 cord slices within injured groups midway along the length of the tissue slices using two sterile
169 scalpel blades #10 (Swann-Morton, England) attached to a scalpel handle. These blades were 460
170 μm distance apart. Spinal cord slices were fixed with 4% PFA at day 3 and day 10 post injury (3
171 spinal cord tissue slices per time point in the control group and 3 spinal cord tissue slices per time
172 point in the injured group).

173

174 **Spinal cord contusion injury model**

175 Longitudinal tissue slices were prepared as detailed in the methods section above and spinal cord
176 tissue slices were pooled together in a petri dish. The tissue slices were then transferred to a 30
177 mm diameter cell culture inserts (1 slice per insert) and cultured at 37°C in a 5% humidified CO₂
178 atmosphere in 6 well trays containing 1ml spinal cord slice culture medium. After 4 days in
179 culture, the tissue slices were separated into a control group (uninjured, 6 slices) and injured group
180 (6 slices). In the injury group, a contusion injury was performed on the slices midway along the
181 length of the spinal cord slices using an Infinite Horizon (IH) Impactor device (Precision Systems
182 and Instrumentation, USA). A sterile mouse impactor rod with a 1.25mm diameter tip was dropped
183 onto the spinal cord slices at a force of 50 kilodynes (kdyn). The spinal cord slices on the inserts
184 were positioned in the centre of the platform and aligned parallel to the position of the impactor
185 rod so as to ensure the rod hit the spinal cord slices. The impactor rod was lowered to 5 mm above
186 the slices prior to injury. Spinal cord slices were fixed with 4% PFA at day 3 and day 10 post injury
187 (3 spinal cord tissue slices per time point in the control group and 3 spinal cord tissue slices per
188 time point in the injured group).

189

190 **Cell viability assay**

191 Control and injured slices from each SCI model were subjected to dual staining for dead cells using
192 PI (Invitrogen, UK) and live cells using FDA (Sigma Aldrich, Ireland). For each injury model,
193 three control and three injured spinal cord slices were examined at 3 days post injury and 10 days
194 post injury. A scalpel blade was used to cut around the edge of the insert mesh in order to remove
195 the insert mesh (containing the spinal cord tissue slices) from the insert ring. Each insert mesh
196 containing the spinal cord tissue slices (2 mm x 2 mm) could fit inside the 24 well tray wells. The
197 tissue slices on insert meshes were washed with 1X PBS three times (5 mins per wash). The slices
198 were incubated with 50 µg/ml PI and 50 µg/ml FDA for 30 seconds at room temperature. The
199 slices were then inverted and placed into 35 mm glass bottom dishes (WillCo Well BV,
200 Netherlands) in 500µl 1X PBS during confocal imaging.

201

202 **Imaging**

203 Images were captured at 10X and 20X magnifications using an Andor spinning disc confocal
204 microscope (Andor Technology Ltd, UK). To examine the stained cells, confocal z-stack images
205 were captured 1 µm apart from the top to the bottom of the spinal cord slices. The red and green
206 channels were used to visualize stained cells at 488 nm and 561 nm emission wavelength
207 respectively. All the imaging was carried out using the same exposure time and emission gain for
208 all the spinal cord slices. One image per slice was obtained from control and one image per slice
209 from injured slices for each animal model.

210

211 **Image analysis**

212 Image analysis was performed to measure the FDA and PI staining. In the uninjured/control tissue
213 slices the central region of the spinal cord tissue slices was examined. In the injured slices a scar
214 zone, defined as a zone that fell in 100 μm radius from the edge of the lesion, was examined. For
215 each image captured, 6 regions on the image were magnified and examined. All the images were
216 prepared and examined at 120% magnification from the original image (100%). A square point
217 grid was placed randomly on the top of the images using computer-generated grids and this grid
218 was used to count the number of points hitting labelled cells. The entire field of view was counted
219 and recorded in Microsoft Excel 2016 (Microsoft Office, USA). Cells were counted positive if
220 the cells lay on intersection points on the grid. All the images were counted with the help of the
221 ImageJ Cell Counter tool. The cells were counted if they stained red (dead cells) and green (live
222 cells). ImageJ software was used to split the two channels and these were measured separately
223 using the de-interleave ImageJ editing tool. The images were inverted to black and white and
224 contrast/brightness levels were adjusted. The average number of cells stained with FDA and PI
225 was calculated in the projected confocal image stacks.

226

227 **Statistics**

228 All data collected was saved in Microsoft Excel 2016 (Microsoft Office, USA). The mean number
229 of live and dead cells was calculated in each image and the results were expressed as mean \pm
230 standard error of the mean (SEM). All the results were illustrated using Graphpad Prism software
231 (Prism 7, USA). Statistical analysis was carried out using Minitab software (Minitab
232 Incorporation, USA). To test for differences between the parameters examined Two-way Analysis

233 of Variance (ANOVA) were performed followed by Multiple comparison Tukey's test. Statistical
234 significance was set at probability $(p) \leq 0.05$.

235

236 **RESULTS**

237 Examination of all *ex vivo* SCI models showed more live cells than dead cells in both control and
238 injured spinal cord slices at each time point. Cell viability was examined within control and injured
239 spinal cord slices at day 3 and day 10 following stab injury (Figure 1A-D). The number of FDA
240 and PI stained cells was counted in the projected confocal image stacks (Figure 1E). When the
241 control and injured groups were compared to each other, higher levels of dead cells were observed
242 in injured slices compared to control slices at both time points post-injury and an increase (non-
243 significant) was also observed in live cells in injured slices compared to control slices (Figure 1E).
244 There was no difference in the numbers of cells when cells were examined between day 3 and 10.

245 In contusion injured spinal cord slices the FDA and PI stained cells were observed (Figure
246 2A-D). Some of the live cells at the lesion site appeared to resemble neurons (see Figure 2D).
247 Immunohistochemical staining for markers of neurons confirmed the presence of many axons at
248 the edge of the lesion site (Supplementary figure 1). Similar cell viability findings were observed
249 in the contused spinal cord slices as those observed in stab injured slices, with a higher levels of
250 dead cells observed in injured slices at both time points compared to control and no change
251 observed over time (Figure 2E).

252 In the transection injury model cell viability was observed at each time point (Figure 3A-
253 D). The proportion of dead cells was higher in transection injured slices than in the control slices
254 at day 3 post-injury with no change observed at day 10 (Figure 3E).

255

256 **DISCUSSION**

257 Cell viability within three *ex vivo* models of rat SCI was investigated here at day 3 and day
258 10 post injury. These *ex vivo* models support the 3R's concept of replacement, reduction and
259 refinement of animal use in SCI research. Observation of cellular changes in *ex vivo* slices allows
260 heterogeneous cell populations to be studied. Neurons and supporting cells are maintained with
261 3-dimensional connections within OSCs (Doussau *et al.*, 2017). In OSCs, one can manipulate
262 treatment strategies to observe the effect of treatments in 3-dimensional microenvironments.
263 Viability of cells in OSCs is a very important parameter to consider when culturing *ex vivo* slice
264 cultures, as cell viability indicates whether the slices are healthy and reliable enough for
265 experimentation. In this study, dual staining using FDA and PI was carried out to examine cell
266 viability within spinal cord slices over 10 days in culture. The 10 day time period allowed
267 investigation of how the environment changes following SCI in *ex vivo* OSCs. This time window
268 was similar to that of other researchers who examined the primary and secondary mechanisms of
269 cell death following *ex vivo* injury (Cho *et al.*, 2009; Gerardo-Nava *et al.*, 2014). We have also
270 investigated secondary injury mechanisms such as scarring in these model systems (data submitted
271 for publication).

272 The selection of the slices used in this study, either transverse slices for use in the stab
273 injury model or longitudinal for use in the transection or contusion injury model, was carefully
274 carried out. An attempt was made to have an equal proportion of both white and grey matter within
275 the slices. In our hands, we managed to obtain eight good slices from one spinal cord. Weightman
276 *et al.* (2014) recommended that the best strategy for selection of slices was to discard the extreme

277 lateral margins of the spinal cord due to presence of fragmented tissue and that the slices should
278 be examined on a dissecting microscope to confirm their intactness (Weightman *et al.*, 2014).

279 In all three *ex vivo* SCI models, the slices showed more live cells than dead cells over the
280 10 days in culture, with higher cell viability in control slices compared to injured slices. These
281 viable cells may be resident cells that have survived the injury, newly generated cells from
282 proliferating cells within the tissue slice and/or cells that have migrated into the slice from adjacent
283 regions. The FDA and PI stains were not specific to any particular cell type, however, we observed
284 some FDA-tagged live cells that appeared like neurons in Figure 3D. The survival of neurons is a
285 major challenge in OSCs. Since the OSCs are an axotomised system, the neurons lose their target
286 innervation and this later causes neuronal death (Humpel, 2015). However, some of the neurons
287 in the OSCs maintain short axonal connections to other neurons, therefore, the axotomy allows
288 one to study neuronal sprouting and reactive synaptogenesis as shown by Gähwiler *et al.* (1997)
289 in hippocampal slices. The contusion injury model showed an increase (albeit non-significant) in
290 live cells between day 3 and day 10 (Figure 2E), which may be due to the difference in the inflicted
291 injury itself as no difference in cell viability was observed between time points in the
292 stab/transection injury models. In our study, we used spinal cord slices derived from P4 rat pups
293 for both transverse and longitudinal oriented slices. It has been reported that neurons are more
294 stable in OSCs when isolated from P6 or younger aged pups, as neurons tend to be more variable
295 with increased age and decline in culture (Bonnici and Kapfhammer, 2008).

296 The contusion model is the most clinically relevant model to human SCI (Cheriyian *et al.*,
297 2014). This model is relevant to investigate the pathophysiology following acute injury. We
298 isolated longitudinal spinal cord slices and induced a contusion injury using the IH impactor
299 device. Our results concur with other studies using the same setting of 50-kdyn force impact and

300 mouse impactor tips indicating a moderate injury of contusion injury (Bastien *et al.*, 2015). After
301 3 days and 10 days in culture, the high numbers of live cells in the slices indicated the cells survived
302 after the impact, although dead cells were also observed (Figure 2E).

303 The idea of using slice cultures is to eliminate confounding factors found *in vivo*, thus
304 helping to elucidate the mechanisms underlying a mechanically induced trauma. The OSC model
305 appears to reproduce much of the post traumatic events including acute and secondary injury
306 mechanisms (Krassioukov *et al.*, 2002, Pinkernelle *et al.*, 2013, Pohland *et al.*, 2015, Weightman
307 *et al.*, 2014). It serves to control the extracellular environment and has the promise of lower
308 economical cost and faster discovery (Morrison *et al.*, 1998). However, the use of *ex vivo* culture
309 system is subjected to some limitations. First, this culture system does not have any blood flow
310 within capillaries. Therefore, the role of monocytes derived from blood circulation following
311 injury cannot be studied in this *ex vivo* system. The accumulation of microglia/macrophages occurs
312 at the edges of slices due to damage caused by the dissection and tissue chopping procedures.
313 However, we optimised our culture protocol by delaying any treatment until day 4 post injury to
314 avoid the involvement of immune cells activated during the tissue harvest procedure. Another
315 limitation to the use of OSCs is that the cells within the slices lose their target innervation as the
316 slices are an axotomized system (Humpel, 2015).

317 In summary, all the *ex vivo* models of SCI presented here have fulfilled the 3R's concept
318 of replacement, reduction and refinement of animal use in SCI research models. Each model is a
319 consistent, easily reproducible and graded injury that represents SCI pathology. Cell viability
320 appeared robust within these OSCs, albeit with a reduction in live cells observed over time in
321 culture within the stab and transection models. These *ex vivo* model systems are very useful for
322 testing potential treatments before moving to larger studies involving animals.

323

324 **ACKNOWLEDGEMENTS**

325 The authors acknowledge the facilities, scientific and technical assistance (Mr Mark
326 Canney and Dr Kerry Thompson) of the Centre for Microscopy and Imaging at the
327 National University of Ireland, Galway (www.imaging.nuigalway.ie), a facility which is
328 co-funded by the Irish Government's Programme for Research in Third Level Institutions, Cycles
329 4 and 5, National Development Plan 2007-2013. Funding for this project was provided by the
330 Malaysia Ministry of Education and the College of Medicine, Nursing and Health Science at NUI
331 Galway. The authors declare that there is no conflict of interest.

332

333 **AUTHOR CONTRIBUTIONS**

334 Azim Patar: contributed to concept/design, acquisition of data, data analysis/interpretation,
335 drafting of the manuscript, revision of the manuscript and approval of the article

336 Peter Dockery contributed to data analysis/interpretation and approval of the article

337 Linda Howard contributed to concept/design, data analysis/interpretation, drafting of the
338 manuscript, critical revision of the manuscript and approval of the article.

339 Siobhan S. McMahon contributed to concept/design, data analysis/interpretation, drafting of the
340 manuscript, critical revision of the manuscript and approval of the article.

341

342 **REFERENCES**

- 343 Adamchik Y, Frantseva MV, Weisspapir M, Carlen PL, Perez Velazquez JL (2000) Methods to induce primary
344 and secondary traumatic damage in organotypic hippocampal slice cultures. *Brain Res Brain Res*
345 *Protoc*, **5**, 153-8.
- 346 Bastien D, Bellver Landete V, Lessard M, et al. (2015) IL-1alpha Gene Deletion Protects Oligodendrocytes
347 after Spinal Cord Injury through Upregulation of the Survival Factor Tox3. *J Neurosci*, **35**, 10715-
348 30.
- 349 Beattie MS, Hermann GE, Rogers RC, Bresnahan JC (2002) Cell death in models of spinal cord injury. *Prog*
350 *Brain Res*, **137**, 37-47.
- 351 Bonnici B, Kapfhammer JP (2008) Spontaneous regeneration of intrinsic spinal cord axons in a novel spinal
352 cord slice culture model. *Eur J Neurosci*, **27**, 2483-92.
- 353 Cheriyan T, Ryan DJ, Weinreb JH, et al. (2014) Spinal cord injury models: a review. *Spinal Cord*, **52**, 588-
354 95.
- 355 Cho JS, Park HW, Park SK, et al. (2009) Transplantation of mesenchymal stem cells enhances axonal
356 outgrowth and cell survival in an organotypic spinal cord slice culture. *Neurosci Lett*, **454**, 43-8.
- 357 Doussau F, Dupont JL, Neel D, Schneider A, Poulain B, Bossu JL (2017) Organotypic cultures of cerebellar
358 slices as a model to investigate demyelinating disorders. *Expert Opin Drug Discov*, **12**, 1011-1022.
- 359 Gähwiler BH, Capogna M, Debanne D, McKinney RA, Thompson SM (1997) Organotypic slice cultures: a
360 technique has come of age. *Trends in Neurosciences*, **20**, 471-477.
- 361 Gerardo-Nava J, Hodde D, Katona I, et al. (2014) Spinal cord organotypic slice cultures for the study of
362 regenerating motor axon interactions with 3D scaffolds. *Biomaterials*, **35**, 4288-96.
- 363 Gerardo-Nava J, Mayorenko, II, Grehl T, Steinbusch HW, Weis J, Brook GA (2013) Differential pattern of
364 neuroprotection in lumbar, cervical and thoracic spinal cord segments in an organotypic rat model
365 of glutamate-induced excitotoxicity. *J Chem Neuroanat*, **53**, 11-7.
- 366 Hashemian S, Marschinke F, Af Bjerken S, Stromberg I (2014) Degradation of proteoglycans affects
367 astrocytes and neurite formation in organotypic tissue cultures. *Brain Res*, **1564**, 22-32.
- 368 Humpel C (2015) Organotypic brain slice cultures: A review. *Neuroscience*, **305**, 86-98.
- 369 Kennedy HS, Jones C, 3rd, Caplazi P (2013) Comparison of standard laminectomy with an optimized
370 ejection method for the removal of spinal cords from rats and mice. *J Histotechnol*, **36**, 86-91.
- 371 Kim HM, Lee HJ, Lee MY, Kim SU, Kim BG (2010) Organotypic spinal cord slice culture to study neural
372 stem/progenitor cell microenvironment in the injured spinal cord. *Exp Neurol*, **19**, 106-13.
- 373 Krassioukov AV, Ackery A, Schwartz G, Adamchik Y, Liu Y, Fehlings MG (2002) An in vitro model of
374 neurotrauma in organotypic spinal cord cultures from adult mice. *Brain Res Brain Res Protoc*, **10**,
375 60-8.
- 376 McCaughey EJ, Purcell M, Barnett SC, Allan DB (2016) Spinal Cord Injury Caused by Stab Wounds:
377 Incidence, Natural History, and Relevance for Future Research. *J Neurotrauma*, **33**, 1416-21.
- 378 Morrison B, 3rd, Saatman KE, Meaney DF, McIntosh TK (1998) In vitro central nervous system models of
379 mechanically induced trauma: a review. *J Neurotrauma*, **15**, 911-28.
- 380 O'Neill S, McKinstry CS, Maguire SM (2004) Unusual stab injury of the spinal cord. *Spinal Cord*, **42**, 429-
381 430.
- 382 Pellowska M, Stein C, Pohland M, et al. (2015) Pharmacokinetic properties of MH84, a gamma-secretase
383 modulator with PPARgamma agonistic activity. *J Pharm Biomed Anal*, **102**, 417-24.
- 384 Pinkernelle J, Fansa H, Ebmeyer U, Keilhoff G (2013) Prolonged minocycline treatment impairs motor
385 neuronal survival and glial function in organotypic rat spinal cord cultures. *PLoS One*, **8**, e73422.
- 386 Pohland M, Glumm R, Stoenica L, et al. (2015) Studying axonal outgrowth and regeneration of the
387 corticospinal tract in organotypic slice cultures. *J Neurotrauma*.

388 Ravikumar M, Jain S, Miller RH, Capadona JR, Selkirk SM (2012) An organotypic spinal cord slice culture
389 model to quantify neurodegeneration. *J Neurosci Methods*, **211**, 280-8.
390 Sieg F, Wahle P, Pape HC (1999) Cellular reactivity to mechanical axonal injury in an organotypic in vitro
391 model of neurotrauma. *J Neurotrauma*, **16**, 1197-213.
392 Steward O, Willenberg R (2017) Rodent spinal cord injury models for studies of axon regeneration. *Exp*
393 *Neurol*, **287**, 374-383.
394 Suzuki M, Klein S, Wetzel EA, et al. (2010) Acute glial activation by stab injuries does not lead to overt
395 damage or motor neuron degeneration in the G93A mutant SOD1 rat model of amyotrophic
396 lateral sclerosis. *Exp Neurol*, **221**, 346-52.
397 Sypecka J, Koniusz S, Kawalec M, Sarnowska A (2015) The organotypic longitudinal spinal cord slice culture
398 for stem cell study. *Stem Cells Int*, **2015**, 471216.
399 Weightman AP, Pickard MR, Yang Y, Chari DM (2014) An in vitro spinal cord injury model to screen
400 neuroregenerative materials. *Biomaterials*, **35**, 3756-65.

401

402

403 **FIGURE LEGENDS**

404 **Figure 1: Live dead assay assessment in stab injured spinal cord *ex vivo* slices.**

405 Photomicrographs show dual staining for live cells with FDA (green) and dead cells with PI (red)
406 at day 3 (A, B) and day 10 (C, D) in control and stab injured slices respectively. Graph shows the
407 number of live and dead cells in the control and injured spinal cord slices (E). Mean \pm SEM. The
408 mean differences were analysed using Two-way ANOVA. n=3 litters (12 pups per litter) which
409 relates to 6 slices per control group per time-point and 6 slices per injured group per time-point for
410 each litter. + = $p \leq 0.05$. Scale bar = 200 μ m

411

412 **Figure 2: Live dead assay assessment in contusion injured spinal cord *ex vivo* slices.**

413 Photomicrographs show dual staining for live cells with FDA (green) and dead cells with PI (red)
414 at day 3 (A, B) and day 10 (C, D) in control and contusion injured slices respectively. Graph shows
415 the number of live and dead cells in the control and injured spinal cord slices (E). Mean \pm SEM.
416 The mean differences were analysed using Two-way ANOVA. n=3 litters (12 pups per litter)
417 which relates to 6 slices per control group per time-point and 6 slices per injured group per time-
418 point for each litter. + = $p \leq 0.05$. * =injury site; Scale bar = 200 μ m

419

420 **Figure 3: Live dead assay assessment in transection injured spinal cord *ex vivo* slices.**

421 Photomicrographs show dual staining for live cells with FDA (green) and dead cells with PI (red)
422 at day 3 (A, B) and day 10 (C, D) in control and transection injured slices respectively. Graph
423 shows the number of live and dead cells in the control and injured spinal cord slices (E). Mean \pm
424 SEM. The mean differences were analysed using Two-way ANOVA. n=3 litters (12 pups per litter)

425 which relates to 6 slices per control group per time-point and 6 slices per injured group per time-
426 point for each litter. + = $p \leq 0.05$. * =injury site; Scale bar = 200 μm .

427

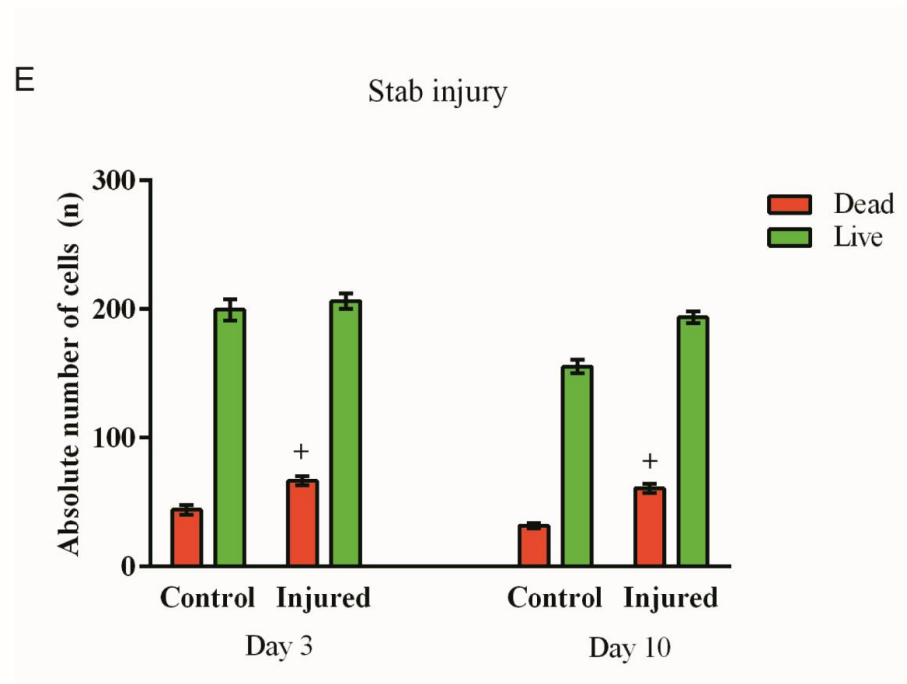
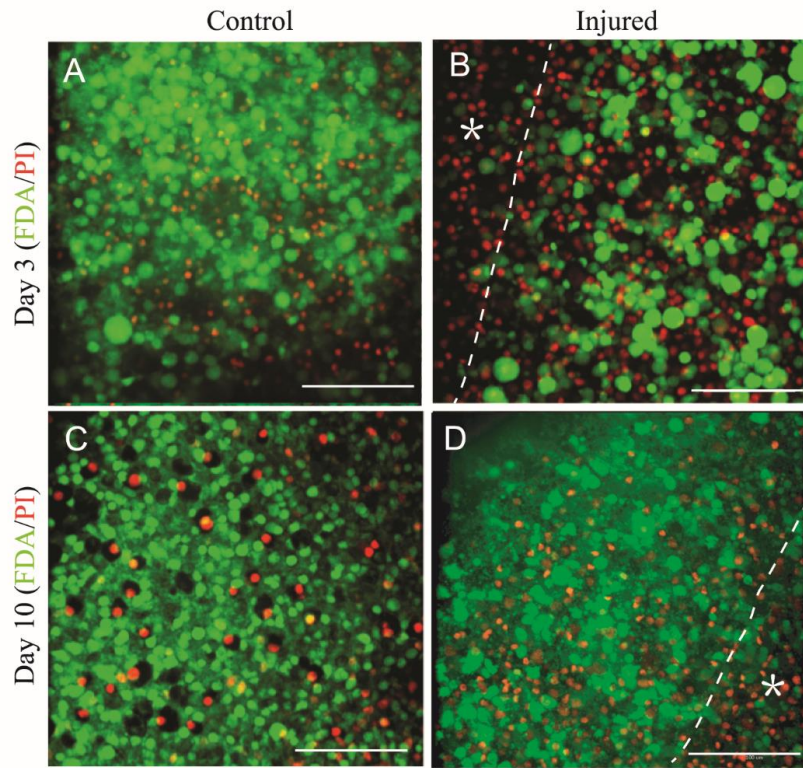
428 **Supplementary figure 1: Distribution of white matter and gray matter in contused tissue**
429 **slices.** Photomicrographs show dual immunostaining of β III Tubulin (neurofilaments) and NeuN
430 (nuclei of neurons) on day 3. Dashed line separates the IZ and tissue region near IZ; White asterisk,
431 IZ= injury zone; * =injury site; scale bar = 200 μm .

432

433

434

Figure 1



435

436

Figure 2

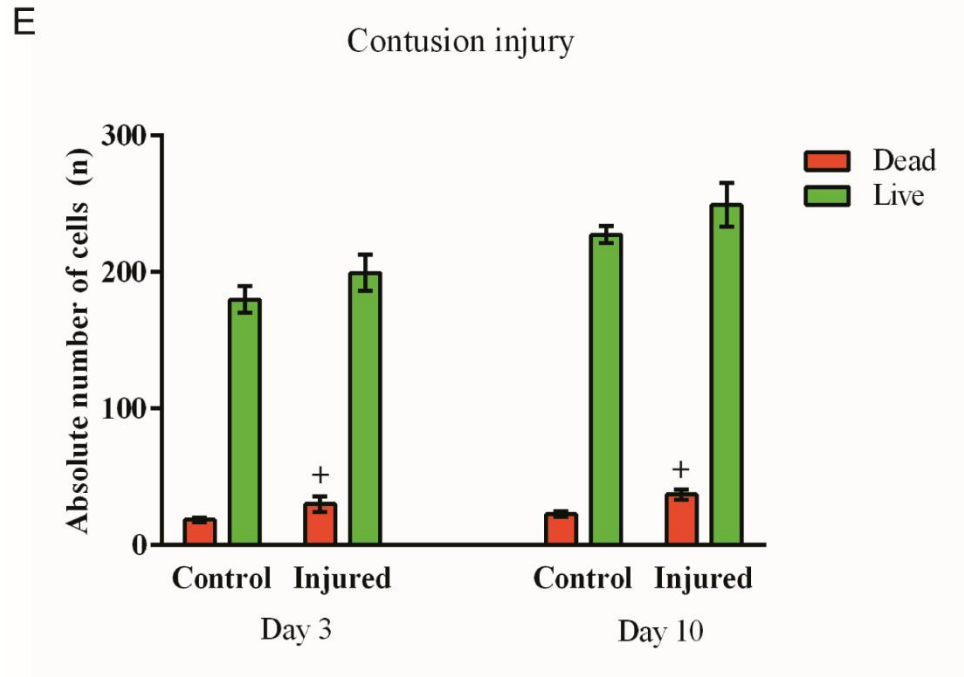
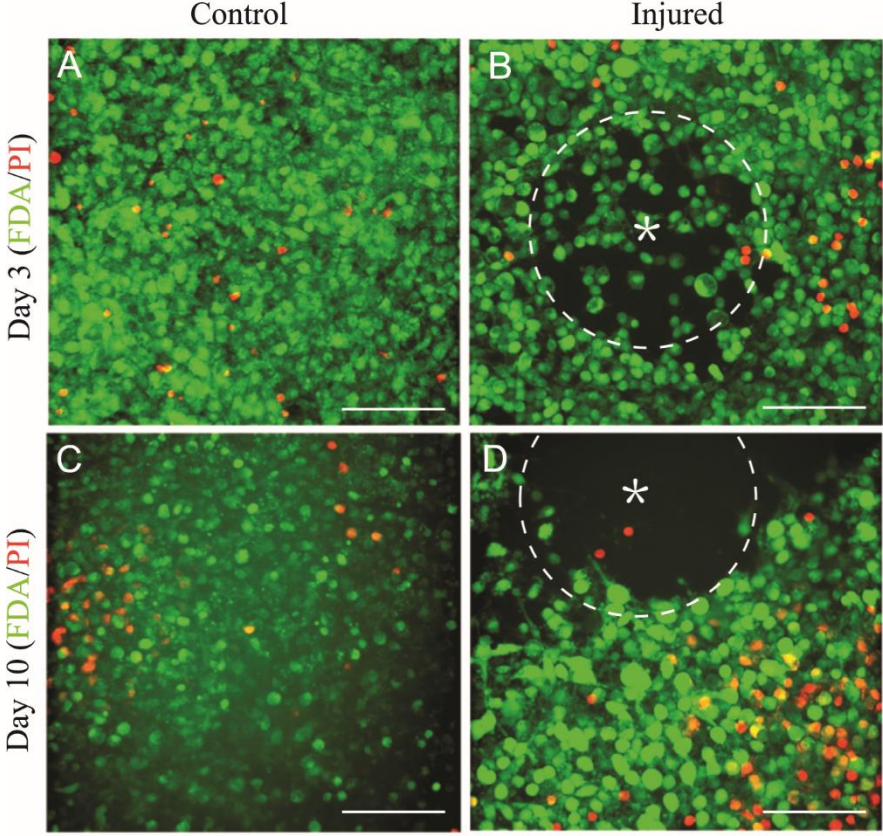
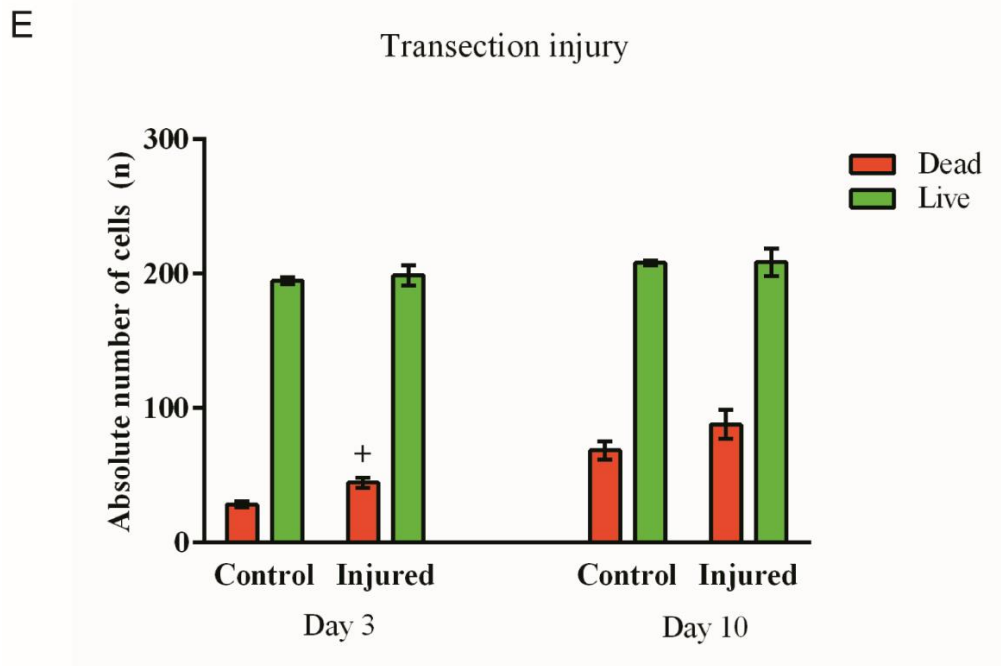
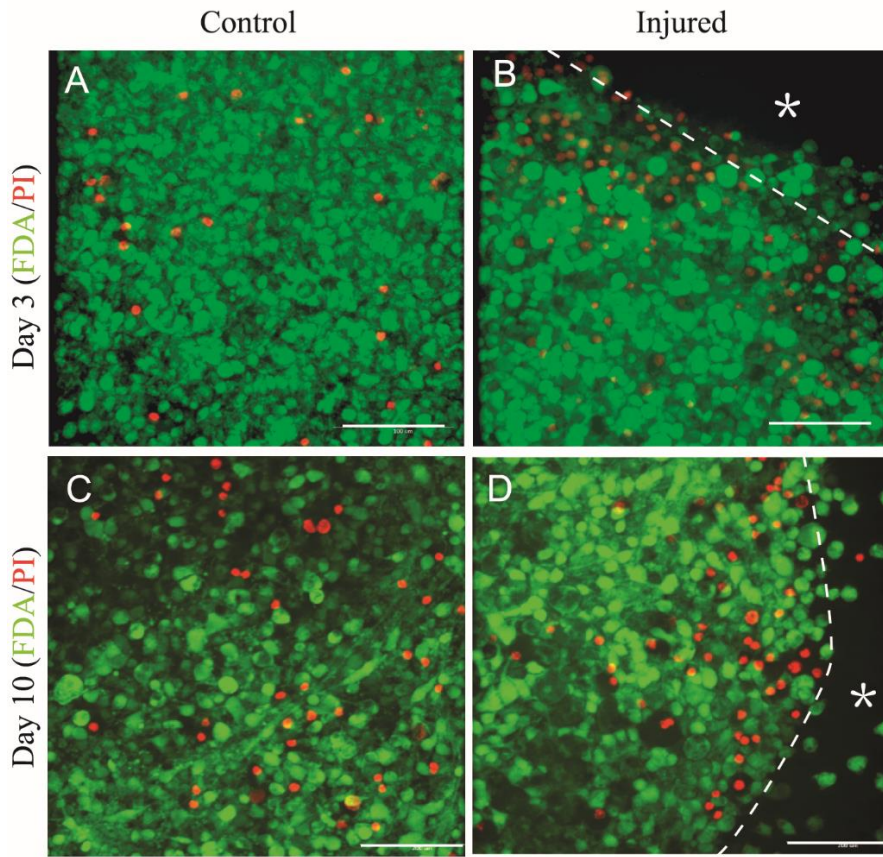


Figure 3



Supplementary figure 1

